Novel pharmacodynamic biomarkers for MYCN protein and PI3K/AKT/mTOR pathway signaling in children with neuroblastoma

Authors and affiliations:

Jennifer R. Smith[a,#], Lucas Moreno[a,b,c,#], Simon P. Heaton[a], Louis Chesler[a,b], Andrew D.J. Pearson[a,b] and Michelle D. Garrett[a,d,*]

[a] Divisions of Clinical Studies and Cancer Therapeutics, The Institute of Cancer Research, London, SM2 5NG, United Kingdom.

[b] Children's and Young People's Unit, Royal Marsden NHS Foundation Trust, Sutton, SM2 5PT, United Kingdom.

[c] CNIO, Spanish National Cancer Research Centre, Melchor Fernandez Almagro 3, 28029 Madrid, Spain.

[d] School of Biosciences, University of Kent, Canterbury, Kent, CT2 7NJ, United Kingdom.

[#] Equal contribution

***Corresponding author:**

Michelle D. Garrett,

School of Biosciences,

University of Kent,

Canterbury,

Kent,

CT2 7NJ

United Kingdom

Phone: +44 (0)1227 816140

Email: m.d.garrett@kent.ac.uk

Abstract

There is an urgent need for improved therapies for children with high-risk neuroblastoma where survival rates remain low. *MYCN* amplification is the most common genomic change associated with aggressive neuroblastoma and drugs targeting PI3K/AKT/mTOR, to activate MYCN oncoprotein degradation, are entering clinical evaluation. Our aim was to develop and validate pharmacodynamic (PD) biomarkers to evaluate both proof of mechanism and proof of concept for drugs that block PI3K/AKT/mTOR pathway activity in children with neuroblastoma. We have addressed the issue of limited access to tumor biopsies for quantitative detection of protein biomarkers by optimizing a three-color fluorescence activated cell sorting (FACS) method to purify CD45-/GD2+/CD56+ neuroblastoma cells from bone marrow. We then developed a novel quantitative measurement of MYCN protein in these isolated neuroblastoma cells, providing the potential to demonstrate proof of concept for drugs that inhibit PI3K/AKT/mTOR signaling in this disease. In addition we have established quantitative detection of three biomarkers for AKT pathway activity (phosphorylated and total AKT, GSK3β and P70S6K) in surrogate platelet-rich plasma (PRP) from pediatric patients. Together our new approach to neuroblastoma cell isolation for protein detection and suite of PD assays provides for the first time the opportunity for robust, quantitative measurement of protein-based PD biomarkers in this pediatric patient population. These will be ideal tools to support clinical evaluation of PI3K/AKT/mTOR pathway drugs and their ability to target MYCN oncoprotein in upcoming clinical trials in neuroblastoma.

Keywords:

Neuroblastoma

MYCN

AKT

Pharmacodynamic

Biomarker

Abbreviations

FACS; Fluorescence activated cell sorting

FCS; Fetal Calf Serum

PBMC; Peripheral blood mononuclear cells

PD; Pharmacodynamic

PRP; Platelet-rich plasma

1. Introduction

Neuroblastoma, a malignancy originating in the sympathetic nervous system, is the most frequent extra-cranial solid tumor in children. Despite intensification of multimodality treatment, the outcome for children with high-risk disease (metastatic or *MYCN* amplified) remains poor. Sixty per cent of neuroblastoma patients experience relapse, and survival after relapse is only 8% (London et al., 2011). There is an urgent need to develop new drugs which can be fast-tracked into frontline therapy to improve cure rates for patients with high-risk disease and to decrease toxicity in long-term survivors (Barone et al., 2013).

Amplification of *MYCN* is one of few genetic abnormalities in neuroblastoma affecting 20% of patients and is more common in high-risk cases (Brodeur et al., 1984). *MYCN* amplification is the strongest genetic alteration linked to poor prognosis in neuroblastoma (Seeger et al., 1985) and promotes metastatic behavior (Benard, 1995). Metastasis is seen in the majority (70%) of patients with high-risk neuroblastoma at the time of diagnosis (Maris et al., 2007) with the most common sites being bone marrow, bone and lymph nodes (DuBois et al., 1999). Mounting evidence for the role of MYCN in driving neuroblastoma (Huang and Weiss, 2013) has led to several therapeutic strategies to target this oncoprotein, (reviewed in (Barone et al., 2013)). Direct pharmacological inhibition of MYCN function through blockade of MYCN/MAX interactions (Zirath et al., 2013) is challenging and alternate strategies have included drugs which indirectly modulate MYCN e.g. BET bromodomain inhibitors that block *MYCN* transcription (Puissant et al., 2013) and inhibiting pathways that regulate stabilization of MYCN protein (Gustafson and Weiss, 2010). MYCN stability is tightly regulated by phosphorylation on residues T58/S62 which block its proteasomal degradation (Vervoorts et al., 2006). The PI3K/AKT/mTOR pathway directly regulates phosphorylation of MYCN, maintaining expression of active MYCN protein, and several inhibitors of this pathway have been shown to cause degradation of MYCN protein (Chesler et al., 2006; Johnsen et al., 2008).

The PI3K/AKT/mTOR pathway is a high priority target in pediatric cancer for several reasons. On the basis of extensive pre-clinical evidence, inhibition of this pathway is predicted to be clinically efficacious in: i) MYCN-driven tumors, including neuroblastoma, medulloblastoma and rhabdomyosarcoma with aberrant amplification, expression or stabilization of MYCN oncoprotein, ii) tumors with aberrant activation of the PI3K/AKT/mTOR pathway (Opel et al., 2007) and, iii) tumors with intrinsic PI3K pathway activating mutations (*PI3KCA, AKT*) or deletions (*PTEN*), although these generally occur less frequently in pediatric than in adult cancers (Dam et al., 2006; Izycka-Swieszewska et al., 2010; Moritake et al., 2001). In neuroblastoma and medulloblastoma, pharmacologic inhibition of the PI3K/AKT/mTOR pathway in genetically engineered murine models has shown antitumor effects mediated by destabilization of MYCN oncoprotein (Chanthery et al., 2012; Pei et al., 2012). Inhibitors of PI3K, PI3K/TORC, TORC and AKT are being evaluated in adult cancers (Porta et al., 2014) and are entering pediatric development in early phase clinical trials (Fouladi et al., 2014; Geoerger et al., 2012; Gore et al., 2013). In support of these trials, it will be crucial to incorporate pharmacodynamic (PD) biomarkers for inhibition of the PI3K/AKT/mTOR pathway and its target MYCN if we are to effectively prioritize use of these drugs.

One of the key issues, particularly in the development of pediatric biomarkers is to establish assays suitable for use in surrogate tissues (commonly blood) and/or methods to isolate disseminated tumor cells, given that biopsy of primary tumor tissue is uncommon (Ang et al., 2012). This study addresses these needs by building i) methodology to efficiently purify neuroblastoma tumor cells from bone marrow for protein biomarker studies, ii) a quantitative immunoassay to measure MYCN oncoprotein levels in neuroblastoma tumor cells, and iii) a set of quantitative PD biomarker assays that robustly measure PI3K/AKT/mTOR pathway activity in platelet-rich plasma. We demonstrate extensive pre-clinical evaluation of these assays and methods and pilot studies establishing assay performance in samples from

pediatric patients. This suite of assays can now be implemented on forthcoming clinical trials of PI3K/AKT/mTOR pathway inhibitors in children with neuroblastoma.

2. Material and methods

2.1 Cell culture and drug treatment

SHEP neuroblastoma cell lines were obtained under consent of the Bishop Laboratory, University of California at San Francisco Cell Culture Facility, and Kelly, BE2C, IMR32 and SKNAS from the American Type Culture Collection. SHEP+ cells (expressing murine MYCN) were previously reported by us (Chesler et al., 2006). Cell lines had either high MYCN expression (*MYCN* amplified: Kelly, BE2C and IMR32) or no expression of human MYCN protein (SHEP, SHEP+ and SKNAS). Kelly and IMR32 cells were cultured in RPMI media with 10% FCS (PAA Laboratories) and 2mM glutamine (Gibco). All other cell lines were grown in DMEM containing 10% FCS and 2mM glutamine. Cell lines were maintained under a humidified atmosphere at 37°C with 5% CO_2 and cultured for less than 6 months before renewal from early passage frozen stocks. All cell lines were shown to be Mycoplasma-free using a PCR-based assay (Minerva Biolabs) and were SNP genotyped yearly. AZD8055 was purchased from Selleckchem. Cells were treated at the indicated concentrations or with an equivalent volume of DMSO for 3 h before harvesting.

2.2 Patient samples

For isolation of pediatric PRP, blood samples were collected from 24 children with solid tumors aged 1-18 years receiving treatment at Royal Marsden NHS Foundation Trust at a single time point. The 24 adult patient blood samples for PRP isolation were taken at the time of enrolment to Phase I trials (baseline). For isolation of neuroblastoma cells, bone marrow samples were collected in heparinized tubes from 14 pediatric patients treated for neuroblastoma. The study was conducted under Institutional Review Board approval (Royal Marsden Committee for Clinical Research [CCR] numbers 3083 and 3358 for adult and pediatric patients, respectively). For development of the FACS assay, healthy volunteer blood was collected with CCR approval (CCR3073). All participants/legal guardians provided signed informed consent prior to any study related procedures.

2.3 Immunomagnetic separation

Samples were incubated for 20 min with CD45 or CD56 MicroBeads (Miltenyi Biotec) in MACS buffer (Miltenyi Biotec). Immunomagnetic separation of the negative fraction (for CD45 depletion) or the positive fraction (for CD56 selection) was performed in MS columns (Miltenyi Biotec) following the manufacturer's instructions. Pre- and Post- enriched samples were analysed by flow cytometry to calculate the proportion of neuroblastoma cells out of the total nucleated cells (purity) using APC-H7-CD45, PE-GD2 and FITC-CD56 antibodies (BD Bioscience) and BD LSRII flow cytometer (Becton and Dickinson).

2.4 A three-color FACS assay for isolation of neuroblastoma cells from bone marrow

For initial development of this assay, Kelly neuroblastoma cells were spiked into (adult) healthy volunteer blood at two concentrations: high (1.5×10^6 cells) or low (3×10^5 cells) in 6ml whole blood. For patient bone marrow samples, 3-8 ml of bone marrow aspirate was collected. Samples were diluted 1:3 in ice-cold Wash buffer (MACS buffer (Miltenyi Biotec), 5% BSA and protease and phosphatase inhibitors) and the mononuclear cell fraction isolated after layering onto Lymphoprep™ and centrifugation at 800 xg for 25 min. The cells were filtered and washed once and kept chilled. One fraction of the sample was immediately resuspended in Cell Lysis Buffer and frozen at -80ºC whilst the remaining fraction was prepared for fluorescence activated cell sorting (FACS). Samples were incubated for 20 min with APC-H7-CD45, PE-GD2 and FITC-CD56 antibodies (BD Bioscience), washed once and resuspended in 1ml Wash buffer. The cells were analyzed with BD FACSAria cell sorter (Beckton and Dickinson, USA) using FACSDiva software. If CD45-/GD2+/CD56+ cells were identified they were sorted by FACS, along with white blood cells (CD45+/GD2-/CD56-) to be used as a negative control. The sorted cells were pelleted, resuspended in Cell Lysis Buffer and frozen at -80ºC. Dotplots presented were produced using WinMDI software.

2.5 Western blotting

Cells were harvested by scraping, washed once in Phosphate-buffered saline (PBS), then resuspended in Cell Lysis Buffer (Cell Signaling Technology) and incubated for 45 min at 4˚C. The lysed cells were centrifuged at 16,000 xg for 15 min and the supernatant collected. Quantification of protein was performed using BCA protein assay (Thermo Scientific) by comparison with BSA standards. Equal amounts of protein (25µg) were separated by SDS-PAGE using 4-12% Bis-Tris NuPAGE gels (Life Technologies), and transferred onto nitrocellulose membranes. Immunoblotting was performed with the following antibodies: MYCN (Santa Cruz); phospho-AKT (S473) and total AKT (Cell Signaling Technology) and GAPDH (Millipore) using blocking buffer (1X Tris-buffered saline, 1% Tween 20, 5% milk). Blots were exposed to film following incubation with SuperSignal West Pico Chemiluminescent Substrate (Thermo Scientific). Western blots shown are representative of three independent repeats.

2.6 MYCN immunoassay

Immulon2HB 96-well plates were coated with mouse MYCN antibody (Abnova) overnight at 4°C. Wells were washed three times with 0.1% Tween 20 wash buffer and blocked for 1 h with blocking buffer (PBS, 1% milk). Cell lysates were added using equal quantities of protein in 50µl volume per well. Recombinant MYCN protein (Abnova) standards and control Kelly cell lysates were included on each plate for QC. After 2 h incubation at 37°C, wells were washed and rabbit MYCN antibody (Novus Biologicals) added for 1.5 h. Following 3 washes, EU-N1 anti-rabbit antibody (Perkin Elmer) was added (1:1500 in DELFIA Assay Buffer, Perkin Elmer) for 1 h. Three further washes were performed followed by 5 min incubation with DELFIA Enhancement Buffer (Perkin Elmer). Plates were read at 615nm on an Envision 2103 plate reader (Perkin Elmer).

2.7 Measurement of PI3K/AKT/mTOR pathway signals

This methodology has been reported before for analysis of PI3K/AKT/mTOR pathway signals in PRP from adult clinical studies in our laboratory (Arkenau et al., 2014; Banerji et al., 2013; Kumar et al., 2014; Omlin et al., 2012; Yap et al., 2011). In brief, blood samples were collected in 2x 2.7ml BD Vacutainer® tubes with sodium citrate. Plasma was collected after centrifugation for 15 min at 200 xg, 4°C. PhosSTOP (Roche) and Cell Lysis Buffer (Cell Signaling Technology) were added and samples were snap frozen at −80°C. Samples were analyzed for total and phospho-Ser473 AKT, total and phospho-Ser9 GSK3β and total and phospho-Thr421/424 P70S6K using electrochemiluminescence (ECL) immunoassays (Meso Scale Discovery®) in 96-well plate format. For each assay pSer473 AKT and total AKT concentrations were back-calculated from a standard curve of recombinant AKT protein. The accuracy and precision of the assays were monitored using quality control (QC) samples created by spiking three known quantities of recombinant AKT into 10% human plasma. Data analysis was performed using the Meso Scale Discovery Workbench software package (Meso Scale Discovery®) and results reported as ECL counts.

3. Results

3.1 A three-color FACS method to isolate neuroblastoma cells for protein detection

An important step early on in clinical development of a drug is to demonstrate proof of concept. For PI3K/AKT/mTOR inhibitors, detection of MYCN protein loss will validate this concept. As MYCN is not expressed in surrogate tissues, only tumor cells can be used to demonstrate proof of concept. Given the logistical and ethical challenges of repeat tumor biopsies in the pediatric population, and the high occurance of bone marrow metastasis in high-risk neuroblastoma (DuBois et al., 1999; Ladenstein et al., 2010), our first aim was to develop a methodology to enrich neuroblastoma cells from bone marrow aspirates in a form suitable for detection of MYCN protein. Based on the knowledge that neuroblastoma cells are CD45-/GD2+/CD56+ (Swerts et al., 2004), we investigated strategies including positive selection of CD56+ cells or depletion of CD45+ cells from the peripheral blood mononuclear cell (PBMC) fraction of blood using immunomagnetic beads, and fluorescence activated cell sorting (FACS) of CD45-/GD2+/CD56+ cells. To directly compare and optimize these methods we used Kelly cells spiked into adult healthy volunteer whole blood. As shown in Table 1, depletion of CD45 or CD56 positive selection using immunomagnetic columns enriched the purity of neuroblastoma cells by 1.7-fold and 3.9-fold respectively, whereas the FACS-based method reproducibly achieved superior enrichment (5.4-fold). We therefore performed further validation of the triple antibody ($CD45^{APC\text{-}H7}$, $GD2^{PE}$, $CD56^{FITC}$) FACS protocol as our preferred methodology.

Kelly cells were spiked into healthy volunteer blood at two different concentrations: high (1.5×10^6 cells per 6 ml blood) and low (3×10^5 cells per 6 ml blood) and compared to pure Kelly cells or PBMCs from unspiked blood. Neuroblastoma cells were isolated from both high and low spiked samples with similar efficiency using the FACS-based method (Fig. 1A). Enrichment was 71% and 74% for high and low spiked samples, respectively compared with 77% for Kelly cells alone (Fig. 1B) and the percentage of neuroblastoma cells recovered (in

relation to the number of cells spiked) was approximately 30% in all samples (Fig. 1C). The fold enrichment of Kelly cells post-sorting was statistically significant with an average of 8.1-fold for high spiked samples and 33.0-fold for low spiked samples compared to the pre-sorted samples ($p<0.001$ and $p=0.003$, respectively). Together these data suggest that this three-color FACS method can be used to reproducibly isolate neuroblastoma cell line cells with high purity from blood regardless of the initial percentage of cells spiked into the sample.

3.2 Isolation of neuroblastoma cells from patient bone marrow

Having determined that three-color FACS can isolate neuroblastoma cell line cells from spiked healthy volunteer blood, the next step was to confirm that the FACS protocol could be effectively applied to extract tumor cells from bone marrow aspirates. Therefore, a pilot study was set up to collect and process bone marrow samples from patients diagnosed with neuroblastoma (n=14). Firstly, we confirmed that we could detect the presence of CD45-/GD2+/CD56+ cells in 11 bone marrow aspirates analyzed from 7 of the 14 patients (see Table 2). Bone marrow involvement was confirmed independently from bone marrow smears and trephine biopsies, by morphology and immunocytochemistry, for all of the positive samples except those with a very low percentage of CD45-/GD2+/CD56+ cells (Table 2), likely due to multicolor flow cytometry analysis being much more sensitive than routine techniques to detect bone marrow infiltration (Beiske et al., 2005). Importantly, all the samples which we found to be negative for CD45-/GD2+/CD56+ cells also had no detectable neuroblastoma cells by independent clinical laboratory analysis (data not shown) and all samples with >1% tumor cells by flow cytometry were confirmed to have heavy infiltration. Therefore, we were confident that our isolation methodology specifically identifies neuroblastoma cells present in samples.

In bone marrow aspirates with a detectable level of infiltrating neuroblastoma cells we used our three-color FACS methodology to isolate the neuroblasts for PD biomarker analysis (Fig.

2A). The extent of bone marrow involvement was variable between samples with range 0.01 - 15.1% and mean of 3.6% (Fig. 2B). Regardless of the extent of bone marrow infiltration, FACS sorting to enrich for neuroblastoma cells resulted in a similar final purity with a mean of 69.2%±10.6 from six isolated samples from which sufficient cells were collected for additional flow cytometry analysis (Fig. 2B). Therefore, a greater enrichment was achieved in samples with lower levels of tumor cell infiltration (Table 2). The purity of the remaining five isolated samples was not determined due to insufficient cell numbers (≤10,000 cells per sample). Overall, these results verified that FACS is an efficient methodology for enrichment of tumor cells from the bone marrow of neuroblastoma patients.

3.3 A novel immunoassay to detect MYCN protein

We next sought to develop a methodology to accurately and quantitatively measure levels of total MYCN protein in neuroblastoma cells. We used DELFIA®, a well proven robust and sensitive technology to develop a novel in-house immunoassay to measure MYCN protein. We standardized our assay using recombinant MYCN protein, showing a strong linear correlation between protein concentration and europium counts (Fig. 3A). The assay was superior to immunoblotting in sensitivity for detection of MYCN protein with signals above background using ≥0.2µg total protein from Kelly cell lysate (Supplementary Fig. S1).

The specificity for detection of MYCN protein in cell lysates was assessed by evaluating 6 neuroblastoma cell lines. Cell lysates from all *MYCN*-amplified cell lines (BE2C, IMR32 and Kelly) showed high signals in the immunoassay using either 25µg or 10µg total protein, which correlated well with MYCN levels determined by western blotting (Fig. 3B and C). In SHEP+, SHEP and SKNAS cells (lacking human MYCN) signals were equivalent to background (Fig. 3B and C).

Inhibition of PI3K/AKT/mTOR signaling stimulates degradation of MYCN through altered MYCN phosphorylation (Chesler et al., 2006; Johnsen et al., 2008). In Kelly neuroblastoma

cells, MYCN protein was depleted following treatment with the TORC inhibitor AZD8055 in a dose-dependent manner (Fig 3D). Our in-house immunoassay accurately quantified this decrease in MYCN protein expression (Fig. 3E). Taken together, these data provide good pre-clinical validation of the MYCN immunoassay for detection of MYCN protein in neuroblastoma cells prior to and post treatment with inhibitors that target the PI3K/AKT/mTOR pathway.

3.4 Preservation of MYCN protein in FACS isolated neuroblastoma cells

Since a key objective of this study was to be able to measure MYCN protein in neuroblastoma cells isolated from patients, we first needed to confirm whether the levels of the MYCN oncoprotein were preserved throughout the isolation procedure using cultured neuroblastoma cells spiked into healthy volunteer blood. Importantly, Kelly cells that were processed and isolated by FACS immediately after spiking into blood showed similar MYCN signals to Kelly cells alone (Fig. 4A). Performing the processing at 4ºC at all stages preserved protein signals better than processing at room temperature, which resulted in 39.1±6.5% lower signals post-sorting. We also investigated MYCN protein levels in spiked samples that were not processed straightaway (as may happen in a clinical trial situation) and instead stored at 4ºC for 1, 4 or 24 hours. MYCN signals were slightly reduced over time with a significant decrease post-sorting of 35.3% at 24 hours compared with Kelly cells alone that were processed immediately (Fig. 4A), even though the efficiency in isolating Kelly cells remained consistent in samples that were stored on ice before processing (Supplementary fig. 2). These findings indicate that samples should be processed in less than 24 hours and ideally starting within 4 hours of collection.

We next assessed the stability of stored lysates using Kelly cells that were spiked into healthy volunteer blood and isolated by 3-color FACS sorting. The isolated cells were lysed, aliquoted and snap frozen, then either kept on dry ice overnight to simulate sample transportation conditions before being stored at -80ºC, or stored at -80ºC directly. Samples

were thawed for MYCN analysis after different periods of storage. MYCN signals were found to be maintained after 1 week and 4 weeks of storage and were unaffected by temporary storage on dry ice (Fig. 4B).

Based on our stability data we recommend that in order to preserve MYCN protein signals in isolated neuroblastoma cells in multi-site clinical trial setting, bone marrow aspirates should be processed promptly on site to isolate neuroblastoma cells and frozen lysates shipped to a single laboratory site for PD biomarker analysis within one month (Fig. 4C)

3.5 Quantitative measurement of MYCN protein in isolated neuroblastoma cells

We next analyzed MYCN levels in Kelly cells that were spiked into healthy volunteer blood at high and low concentrations. Consistent with the enrichment of neuroblastoma cells (expressing MYCN) in the high and low spiked samples (Fig. 1B), signals for MYCN were increased post-sorting compared with pre-sorted samples (Fig. 4D) showing that the isolation method can effectively be used in combination with MYCN protein measurement in samples with varying numbers of tumor cells.

To further corroborate whether quantification of MYCN protein levels as a pharmacodynamic biomarker is feasible in isolated neuroblastoma cells, Kelly cells were pre-treated with AZD8055 before spiking into healthy volunteer blood and then sorted by FACS. Using equal amounts of total protein in spiked samples and the isolated neuroblastoma cells, samples were analyzed using the MYCN immunoassay. MYCN expression was decreased by AZD8055 in a dose-dependent manner in Kelly cells spiked into blood and importantly, the drug-mediated reduction in MYCN protein was still measurable in the Kelly cells that had been isolated from whole blood (Fig. 4E).

To monitor intra-assay reproducibility and inter-assay reliability, a standard curve was generated using MYCN recombinant protein and quality controls (QCs) were prepared from

Kelly cell lysates and included in each assay. Levels of intra- and inter- assay variation, assessed by coefficient of variation (%CV), were acceptable for each point of the standard curve and the interpolated QCs (Supplementary Fig. S3A-D). MYCN protein concentrations in the QCs were estimated using the standard curve and used to generate acceptance criteria for each QC in the assay (Mean concentration ± 30%). In 5 independent repeats (each using quadruplicate wells) all assays passed according to the 4-6-30 rule (Smolec et al., 2005) demonstrating acceptable assay precision (Supplementary Fig. S3E).

3.6 Analysis of MYCN protein in neuroblastoma cells isolated from patient bone marrow

Next, to establish whether MYCN oncoprotein could be measured in neuroblastoma cells from patients, bone marrow aspirates from 4 patients (patients 6, 8, 11 and 14, Table 2), were subjected to the three-color FACS methodology and the isolated CD45-/GD2+/CD56+ neuroblastoma cells were lysed and analyzed for MYCN protein expression using our in-house immunoassay. We confirmed that MYCN protein was detectable both in the whole mononuclear cell population collected from bone marrow, with an increased level after the FACS isolation procedure, consistent with the enrichment for MYCN-expressing CD45-/GD2+/CD56+ neuroblastoma cells (Fig. 5A and B, patient 8). CD45+/GD2-/CD56- white blood cells that were isolated concurrently with CD45-/GD2+/CD56+ neuroblastoma cells gave signals close to background in the immunoassay, as would be expected in a cell population that does not express MYCN. Analysis of bilateral aspirates (from the same patient) showed good concordance of MYCN expression, suggesting reproducibility of this approach (Fig. 5A and B, patient 8). To further corroborate specificity of the immunoassay for measurement of MYCN protein, we confirmed the expression of MYCN in the same bone marrow sample by western blotting (Fig 5C). Additionally, analysis of MYCN protein levels in three further patients (patients 6, 11 and 14) showed that the highest expression, either pre- or post-sorting, was measured in the *MYCN* amplified patient (Fig. 5D). These data

demonstrate that MYCN protein can be quantitatively measured in bone marrow-resident neuroblastoma cells both before and after enrichment.

3.7 Measurement of PI3K/AKT/mTOR pathway activity in platelet-rich plasma from children

Since a key driver of MYCN stability in neuroblastoma cells is PI3K/AKT/mTOR signaling, we sought to address the need to monitor the activity of this pathway in children with neuroblastoma. We chose to determine the feasibility of using the Meso Scale Discovery® (MSD®) multiplex electrochemiluminescence platform to measure total and phospho-protein signals for AKT, GSK3β and P70S6K, in neuroblastoma cells and also platelet-rich plasma (PRP), the latter as a surrogate tissue. These assays have been validated to meet Good Clinical Practice requirements and have been used by our laboratory to detect PI3K/AKT/mTOR activity in PRP as a surrogate tissue in five adult phase I clinical trials of PI3K/AKT/mTOR inhibitors including MK2206 and AZD5363 (Arkenau et al., 2014; Banerji et al., 2013; Kumar et al., 2014; Omlin et al., 2012; Yap et al., 2011), but have not been evaluated in the pediatric setting until now.

Firstly, we tested whether these assays reliably detect changes in PI3K/AKT/mTOR pathway activity in neuroblastoma cells following treatment with the TORC1/TORC2 inhibitor AZD8055. We confirmed that phospho- AKT, GSK3β and P70S6K signals decreased compared to total levels of each of the biomarkers following 3 h AZD8055 treatment of Kelly neuroblastoma cells (Supplementary Fig. S4A and B). We next looked to see whether the triplex MSD® assays for AKT pathway activity could be used to measure signals of these biomarkers in Kelly neuroblastoma cells, after their isolation from spiked blood by three-color sorting. However, compared with the pre-spiked Kelly cells, levels of all three biomarkers were considerably reduced following this isolation procedure, resulting in an unreliable measurement of AZD8055-mediated inhibition (data not shown). Given that PI3K/AKT/mTOR pathway activity can be measured robustly in PRP, commonly used as a

surrogate normal tissue for PD assessment (Yap et al., 2014), we next investigated whether these assays would be suitable for the detection of these signals in PRP from a pediatric population. Baseline PRP samples from 24 children with solid tumors receiving treatment at our unit were collected and divided into three cohorts (1-4, >4-10 and >10-18 years, n=8/group) for analysis. Supplementary Table S1a shows demographic characteristics of these patients. Baseline signal amplitude and range in PRP was compared to that of 24 adult patients with solid tumors (Supplementary Table S1b) to establish validity of the assay for pediatric patients. Good reproducibility between assays was demonstrated by the inclusion of AKT standards and quality controls (Supplementary Figure S5).

Importantly, all pediatric patient PRP samples had detectable total and phosphorylated AKT, P70S6K and GSK3β protein levels (Fig. 6A and B). The phospho-AKT signal was statistically lower in the pediatric versus adult patient samples ($p=0.022$), whilst both phospho-GSK3β and phospho-P70S6K were significantly higher ($p=0.002$ and $p=0.009$ respectively, Figure 6A). Total AKT and P70S6K levels were not statistically different between adult and pediatric patients ($p>0.05$), whilst total GSK3β was significantly higher in the pediatric patients ($p=0.002$, Figure 6B). Using the ratio of phospho/total levels for each biomarker, the level of activated AKT was again statistically lower in the pediatric versus adult patient samples ($p=0.002$), whilst levels of activated GSK3β and P70S6K were slightly higher in pediatric samples ($p>0.05$ and $p=0.038$, respectively, Fig. 6C). Within the pediatric subset of PRP samples, no significant differences were found in the levels of the three biomarkers according to age group, disease stage, primary tumor type or *MYCN* status ($p>0.05$ by two-tailed t test).

Taken together, these preliminary data indicate that these assays could be used to accurately measure PI3K/AKT/mTOR pathway activity in pediatric PRP as a surrogate tissue, and additionally detect pathway inhibition in cells treated with a drug we propose to

use in clinical evaluation. Therefore, we propose that the MSD® assays are fit-for-purpose to be tested in future clinical trials in children to measure PI3K/AKT/mTOR target engagement.

4. Discussion

Development of pediatric early phase clinical trials with biomarkers utilizing novel anticancer drugs has traditionally lagged behind that of adult cancers. In part this relates to lack of biopsy tissue in children, and to a deficiency in PD assays robust enough to support clinical trials. It is now crucial to develop and implement appropriate PD biomarkers in early phase clinical trials for childhood cancers to ensure that these trials are as informative as possible. Analysis of PD biomarkers has two key objectives: i) to determine whether novel targeted drugs inhibit the expected target(s) in patient tissue (tumor or surrogate) i.e. proof of mechanism, and ii) to ascertain whether modulation of the drug target results in the expected biological downstream effect(s) i.e. proof of concept. PD biomarker assays are therefore valuable components of the pharmacological audit trail to evaluate new molecular targeted drugs (Workman, 2003).

We report for the first time the development of a panel of PD biomarker assays and methodology to isolate metastatic neuroblastoma cells for PD biomarker analysis, these assays are ready to be implemented in early phase clinical trials of agents targeting PI3K, AKT or the mTOR complex and provide the opportunity to demonstrate both proof of mechanism and proof of concept for these agents in neuroblastoma. The rationale for using these classes of inhibitors in neuroblastoma and other MYCN-driven tumors is that the pathway is either dysregulated or mutated in several pediatric malignancies, and that blockade of PI3K/AKT/mTOR will lead to degradation of MYCN protein.

One of the biggest challenges to incorporating PD biomarkers in early pediatric clinical trials remains obtaining suitable tissues, either tumor material or appropriate surrogate tissues (Ang et al., 2012; Gainor et al., 2014). In neuroblastoma, tumor mass at relapse is generally small, localizes to bone or is otherwise inaccessible (e.g. retroperitoneal or mediastinal) and therefore repeated tumor biopsies are challenging. Circulating cell free tumor DNA represents one option for measuring cancer-associated genetic alterations during treatment.

Bone marrow samples are also routinely collected, commonly with detectable tumor infiltration, although the number of cells is variable. Several groups have used immunomagnetic separation methods to isolate neuroblastoma cells from bone marrow samples for genomic or cell surface expression studies (Abbasi et al., 2015; Morandi et al., 2012; Scaruffi et al., 2012; Vandewoestyne et al., 2012). We found this technique to be unsuitable for our purposes as it involved several steps that led to significant cell loss and greater variability and resulted in poorer final purity of neuroblastoma cells than FACS.

Flow cytometry is commonly used for diagnosis and research studies in neuroblastoma but cell sorting has not been applied for pharmacodynamic studies before. Using a three-color FACS-based method we obtained cell suspensions with a high purity for neuroblastoma, with acceptable cell loss and preserved MYCN protein signals when processing was initiated up to 4 hours after sample collection. FACS sorting provides an opportunity for biomarker monitoring in tumor cells themselves from routine bone marrow aspirates without the need for additional biopsies. This methodology has particular importance when tumor cell-specific biomarkers such as MYCN protein are to be measured as there is no alternative option of using surrogate tissues. Therefore, we propose that isolating neuroblastoma cells from bone marrow as a substrate for protein-based PD biomarker assays could be combined with the use of more readily available surrogate tissues (such as PRP) in early clinical trials to provide a fully comprehensive overview of drug-mediated biomarker responses.

Previous pediatric phase I trials of mTOR inhibitors have measured phosphorylation of AKT and S6 kinase in PBMCs using western blotting and/or immunohistochemistry. In the phase I trial of Temsirolimus there was no evidence of a PK/PD relationship as assessed by phosphorylation of AKT, p70S6K or 4EBP1 by western blotting (Spunt et al., 2011). However, in the phase I study of Everolimus, decreases in AKT phosphorylation were detected by western blotting following treatment (Fouladi et al., 2007) and in a phase I trial of Ridaforolimus, inhibition of p4EBP1 was demonstrated for the majority of patients, again by

western blotting (Gore et al., 2013). Although these studies have begun to monitor PD biomarkers in pediatric patients, the traditional histology and immunoblotting methodologies, which have not been specifically optimized for this purpose, have a number of deficiencies e.g. limited and/or unspecified sensitivity, qualitative or semi-quantitative, and no integrated measure of assay performance and reproducibility.

In the pediatric setting where phase I studies may be conducted in 10 or more sites, standard operating procedures for sample collection and processing are vital to ensure that results from multiple sites are comparable (Kinders et al., 2014). Assays require thorough optimization and evaluation to ensure that they are fit-for-purpose and the inclusion of appropriate controls is paramount. We have performed substantial analytic method validation and included standard and quality controls to ensure reliability and reproducibility of PD biomarker assays for PI3K/AKT/mTOR pathway activity and MYCN oncoprotein.

Here we show that the AKT triplex MSD® assays for phospho and total AKT, GSK3β and P70S6K can be used in the pediatric oncology population with several advantages over histology and western blotting techniques. Specifically, these assays provide a quantitative non-invasive measure of three pathway-specific markers simultaneously, thus requiring smaller samples and giving a more reliable measurement of pathway activation. Using these assays, some of the baseline values in pediatric patients were significantly different from those in adults. Further comparing the levels of phospho and total AKT, GSK3β and P70S6K, we found no correlation with age, tumor type, disease stage or *MYCN* status within the pediatric samples. It is difficult to speculate on the reason for the variation in this surrogate tissue between children and adults and indeed whether our results represent genuine differences due to the relatively small sample populations. Most importantly we have determined that the assays are fit-for-purpose in the pediatric setting with signals within the detectable range and provide the opportunity to demonstrate proof of mechanism in clinical trials of drugs that target the PI3K/AKT/mTOR pathway in the pediatric setting

To date, western blotting has remained the gold standard for MYCN protein quantification (Cohn et al., 2000). Here, we present a new immunoassay that will allow the robust measurement of MYCN protein levels in patients receiving MYCN-targeted therapies using smaller samples than western blotting and with the inclusion of appropriate assay controls for performance monitoring. MYCN protein can be measured in bone marrow aspirates from neuroblastoma patients with bone marrow involvement, however due to the high variability in the percentage of tumor cells present, we recommend that neuroblastoma cell enrichment by FACS is performed to allow better comparison of MYCN levels in paired pre-treatment and post-treatment samples in a clinical trial. Additionally, we show that MYCN signals remain stable in lysates, once frozen, for at least 4 weeks, thus providing the opportunity to transport samples to a central laboratory to run the MYCN immunoassay. Measuring changes in MYCN levels during the clinical trials will test the hypothesis developed pre-clinically that PI3K inhibitors exert their antitumor activity in-part via destabilization of MYCN protein and therefore has the potential to deliver proof of concept for these agents (Chesler et al., 2006).

In conclusion, we have provided pre-clinical and clinical validation of assays to measure PI3K/AKT/mTOR pathway signaling and MYCN protein expression as well as a method to isolate neuroblastoma cells for protein biomarker analysis. These PD assays have the potential to deliver both proof of mechanism and proof of concept for new drugs that target the PI3K/AKT/mTOR pathway and are now ready to be implemented as a research endpoint in early clinical trials of these agents in children with neuroblastoma.

Acknowledgements

We acknowledge NHS funding to the NIHR Biomedical Research Centre and funding from ECMC (Experimental Cancer Medicine Centre) Network for the collection of the samples. We thank Prof. Klaus Beiske (University of Oslo) and Dr. Ayad Atra (Royal Marsden NHS Foundation Trust) for their advice with the bone marrow experiments. Many thanks to Ian Titley and Gowri Viiayaraghavan for assistance with flow cytometry, Karen Swales and Shaun Decordova for adult PRP data, and to Giuseppe Barone, Dominik Schrey, Fernando Carceller, Emma Kipps and Jooern Ang and staff at the Children's and Young People's Unit, Royal Marsden NHS Foundation Trust for the collection of samples.

Financial support:

JRS is funded by The Royal Marsden Biomedical Research Centre and Royal Marsden Paediatric Research Fund W91035. LM is funded by the Oak Foundation and SPH is funded through CRUK Medicine grant C347/A15403. ADJP is funded through a Cancer Research UK Life Chair and Programme Grant included within a Cancer Research UK ICR Core Award (C347/A15403) and is supported from the NIHR RM/ICR Biomedical Research Centre. MDG was funded through Cancer Research UK [CUK] programme grant number C309/A11566, and by The Institute of Cancer Research and is currently funded through the University of Kent.

References

Uncategorized References

Abbasi, M.R., Rifatbegovic, F., Brunner, C., Ladenstein, R., Ambros, I.M., Ambros, P.F., 2015. Bone marrows from neuroblastoma patients: an excellent source for tumor genome analyses. Mol Oncol 9, 545-554.

Ang, J.E., Kaye, S., Banerji, U., 2012. Tissue-based approaches to study pharmacodynamic endpoints in early phase oncology clinical trials. Curr Drug Targets 13, 1525-1534.

Arkenau, H., Mateo, J., Lemech, C.R., Infante, J.R., Burris III, H.A., Bang, Y., Eder, J.P., Herbst, R.S., Sharma, S., Chung, H.C., Decordova, S., Swales, K.E., Garrett, M.D., Loftiss, J.I., Durante, M., Russo, M.W., Suttle, B.B., Motwani, M., Kumar, R., De Bono, J.S., 2014. A Phase-I/II, first in human dose escalation study of GSK2636771 in patients (pts) with PTEN deficient advanced tumors., ASCO Annual Meeting.

Banerji, U., Ranson, M., Schellens, J.H.M., Esaki, T., Dean, E., Zivi, A., Van der Noll, R., Stockman, P.K., Marotti, M., Garrett, M.D., Davies, B.R., Elvin, P., Hastie, A., Lawrence, P., Cheung, Y.Y.A., Stephens, C., Tamura, K., 2013. Results of two phase I multicenter trials of AZD5363, an inhibitor of AKT1, 2 and 3: Biomarker and early clinical evaluation in Western and Japanese patients with advanced solid tumors, AACR Annual meeting.

Barone, G., Anderson, J., Pearson, A.D., Petrie, K., Chesler, L., 2013. New strategies in neuroblastoma: Therapeutic targeting of MYCN and ALK. Clin Cancer Res 19, 5814-5821.

Beiske, K., Ambros, P.F., Burchill, S.A., Cheung, I.Y., Swerts, K., 2005. Detecting minimal residual disease in neuroblastoma patients-the present state of the art. Cancer Lett 228, 229-240.

Benard, J., 1995. Genetic alterations associated with metastatic dissemination and chemoresistance in neuroblastoma. Eur J Cancer 31A, 560-564.

Brodeur, G.M., Seeger, R.C., Schwab, M., Varmus, H.E., Bishop, J.M., 1984. Amplification of N-myc in untreated human neuroblastomas correlates with advanced disease stage. Science 224, 1121-1124.

Chanthery, Y.H., Gustafson, W.C., Itsara, M., Persson, A., Hackett, C.S., Grimmer, M., Charron, E., Yakovenko, S., Kim, G., Matthay, K.K., Weiss, W.A., 2012. Paracrine signaling through MYCN enhances tumor-vascular interactions in neuroblastoma. Sci Transl Med 4, 115ra113.

Chesler, L., Schlieve, C., Goldenberg, D.D., Kenney, A., Kim, G., McMillan, A., Matthay, K.K., Rowitch, D., Weiss, W.A., 2006. Inhibition of phosphatidylinositol 3-kinase destabilizes Mycn protein and blocks malignant progression in neuroblastoma. Cancer Res 66, 8139-8146.

Cohn, S.L., London, W.B., Huang, D., Katzenstein, H.M., Salwen, H.R., Reinhart, T., Madafiglio, J., Marshall, G.M., Norris, M.D., Haber, M., 2000. MYCN expression is not prognostic of adverse outcome in advanced-stage neuroblastoma with nonamplified MYCN. J Clin Oncol 18, 3604-3613.

Dam, V., Morgan, B.T., Mazanek, P., Hogarty, M.D., 2006. Mutations in PIK3CA are infrequent in neuroblastoma. BMC Cancer 6, 177.

DuBois, S.G., Kalika, Y., Lukens, J.N., Brodeur, G.M., Seeger, R.C., Atkinson, J.B., Haase, G.M., Black, C.T., Perez, C., Shimada, H., Gerbing, R., Stram, D.O., Matthay, K.K., 1999. Metastatic sites in stage IV and IVS neuroblastoma correlate with age, tumor biology, and survival. J Pediatr Hematol Oncol 21, 181-189.

Fouladi, M., Laningham, F., Wu, J., O'Shaughnessy, M.A., Molina, K., Broniscer, A., Spunt, S.L., Luckett, I., Stewart, C.F., Houghton, P.J., Gilbertson, R.J., Furman, W.L., 2007. Phase I study of everolimus in pediatric patients with refractory solid tumors. J Clin Oncol 25, 4806-4812.

Fouladi, M., Perentesis, J.P., Phillips, C.L., Leary, S., Reid, J.M., McGovern, R.M., Ingle, A.M., Ahern, C.H., Ames, M.M., Houghton, P., Doyle, L.A., Weigel, B., Blaney, S.M., 2014. A phase I trial of MK-2206 in children with refractory malignancies: A Children's Oncology Group study. Pediatr Blood Cancer 61, 1246-1251.

Gainor, J.F., Longo, D.L., Chabner, B.A., 2014. Pharmacodynamic biomarkers: falling short of the mark? Clin Cancer Res 20, 2587-2594.

Geoerger, B., Kieran, M.W., Grupp, S., Perek, D., Clancy, J., Krygowski, M., Ananthakrishnan, R., Boni, J.P., Berkenblit, A., Spunt, S.L., 2012. Phase II trial of temsirolimus in children with high-grade glioma, neuroblastoma and rhabdomyosarcoma. Eur J Cancer 48, 253-262.

Gore, L., Trippett, T.M., Katzenstein, H.M., Boklan, J., Narendran, A., Smith, A., Macy, M.E., Rolla, K., Pediatric Oncology Experimental Therapeutics Investigators, C., Narashimhan, N., Squillace, R.M., Turner, C.D., Haluska, F.G., Nieder, M., 2013. A multicenter, first-in-pediatrics, phase 1, pharmacokinetic and pharmacodynamic study of ridaforolimus in patients with refractory solid tumors. Clin Cancer Res 19, 3649-3658.

Gustafson, W.C., Weiss, W.A., 2010. Myc proteins as therapeutic targets. Oncogene 29, 1249-1259.

Huang, M., Weiss, W.A., 2013. Neuroblastoma and MYCN. Cold Spring Harb Perspect Med 3, a014415.

Izycka-Swieszewska, E., Brzeskwiniewicz, M., Wozniak, A., Drozynska, E., Grajkowska, W., Perek, D., Balcerska, A., Klepacka, T., Limon, J., 2010. EGFR, PIK3CA and PTEN gene status and their protein product expression in neuroblastic tumours. Folia Neuropathol 48, 238-245.

Johnsen, J.I., Segerstrom, L., Orrego, A., Elfman, L., Henriksson, M., Kagedal, B., Eksborg, S., Sveinbjornsson, B., Kogner, P., 2008. Inhibitors of mammalian target of rapamycin downregulate MYCN protein expression and inhibit neuroblastoma growth in vitro and in vivo. Oncogene 27, 2910-2922.

Kinders, R., Ferry-Galow, K., Wang, L., Srivastava, A.K., Ji, J.J., Parchment, R.E., 2014. Implementation of validated pharmacodynamic assays in multiple laboratories: challenges, successes, and limitations. Clin Cancer Res 20, 2578-2586.

Kumar, R., Mateo, J., Smith, A., Khan, K., Ruddle, R., Swales, K.E., Decordova, S., Backholer, Z., Jones, P., Tran, C., Seeramreddi, S., McLeod, R., Yap, T.A., Raynaud, F.I., Garrett, M.D., Banerji, U., 2014. First-in-human, first-in-class Phase 1 study of a novel oral multi-AGC kinase inhibitor AT13148 in patients (pts) with advanced solid tumors, ASCO Annual Meeting.

Ladenstein, R., Valteau-Couanet, D., Brock, P., Yaniv, I., Castel, V., Laureys, G., Malis, J., Papadakis, V., Lacerda, A., Ruud, E., Kogner, P., Garami, M., Balwierz, W., Schroeder, H., Beck-Popovic, M., Schreier, G., Machin, D., Potschger, U., Pearson, A., 2010. Randomized Trial of prophylactic granulocyte colony-stimulating factor during rapid COJEC induction in pediatric patients with high-risk neuroblastoma: the European HR-NBL1/SIOPEN study. J Clin Oncol 28, 3516-3524.

London, W.B., Castel, V., Monclair, T., Ambros, P.F., Pearson, A.D., Cohn, S.L., Berthold, F., Nakagawara, A., Ladenstein, R.L., Iehara, T., Matthay, K.K., 2011. Clinical and biologic features predictive of survival after relapse of neuroblastoma: a report from the International Neuroblastoma Risk Group project. J Clin Oncol 29, 3286-3292.

Maris, J.M., Hogarty, M.D., Bagatell, R., Cohn, S.L., 2007. Neuroblastoma. Lancet 369, 2106-2120.

Morandi, F., Scaruffi, P., Gallo, F., Stigliani, S., Moretti, S., Bonassi, S., Gambini, C., Mazzocco, K., Fardin, P., Haupt, R., Arcamone, G., Italian Cooperative Group for, N., Pistoia, V., Tonini, G.P., Corrias, M.V., 2012. Bone marrow-infiltrating human neuroblastoma cells express high levels of calprotectin and HLA-G proteins. PLoS One 7, e29922.

Moritake, H., Horii, Y., Kuroda, H., Sugimoto, T., 2001. Analysis of PTEN/MMAC1 alteration in neuroblastoma. Cancer Genet Cytogenet 125, 151-155.

Omlin, A.G., Spicer, J.F., Sarker, D., Pinato, D.J., Agarwal, R., Cassier, P.A., Stavraka, C., Blanco, M., Suder, A., Allan, S., Heaton, S., Decordova, S., Pope, L., Prince, J., Noguchi, K., Jones, K., Inatani, M., Shiokawa, R., Banerji, U., Blagden, S.P., 2012. A pharmacokinetic (PK) pharmacodynamic (PD) driven first-in-human study of the oral class I PI3K inhibitor CH5132799, in patients with advanced solid tumors., ASCO Annual Meeting.

Opel, D., Poremba, C., Simon, T., Debatin, K.M., Fulda, S., 2007. Activation of Akt predicts poor outcome in neuroblastoma. Cancer Res 67, 735-745.

Pei, Y., Moore, C.E., Wang, J., Tewari, A.K., Eroshkin, A., Cho, Y.J., Witt, H., Korshunov, A., Read, T.A., Sun, J.L., Schmitt, E.M., Miller, C.R., Buckley, A.F., McLendon, R.E., Westbrook, T.F., Northcott, P.A., Taylor, M.D., Pfister, S.M., Febbo, P.G., Wechsler-Reya, R.J., 2012. An animal model of MYC-driven medulloblastoma. Cancer Cell 21, 155-167.

Porta, C., Paglino, C., Mosca, A., 2014. Targeting PI3K/Akt/mTOR Signaling in Cancer. Front Oncol 4, 64.

Puissant, A., Frumm, S.M., Alexe, G., Bassil, C.F., Qi, J., Chanthery, Y.H., Nekritz, E.A., Zeid, R., Gustafson, W.C., Greninger, P., Garnett, M.J., McDermott, U., Benes, C.H., Kung, A.L., Weiss, W.A., Bradner, J.E., Stegmaier, K., 2013. Targeting MYCN in neuroblastoma by BET bromodomain inhibition. Cancer Discov 3, 308-323.

Scaruffi, P., Morandi, F., Gallo, F., Stigliani, S., Parodi, S., Moretti, S., Bonassi, S., Fardin, P., Garaventa, A., Zanazzo, G., Pistoia, V., Tonini, G.P., Corrias, M.V., 2012. Bone marrow of neuroblastoma patients shows downregulation of CXCL12 expression and presence of IFN signature. Pediatr Blood Cancer 59, 44-51.

Seeger, R.C., Brodeur, G.M., Sather, H., Dalton, A., Siegel, S.E., Wong, K.Y., Hammond, D., 1985. Association of multiple copies of the N-myc oncogene with rapid progression of neuroblastomas. N Engl J Med 313, 1111-1116.

Smolec, J., DeSilva, B., Smith, W., Weiner, R., Kelly, M., Lee, B., Khan, M., Tacey, R., Hill, H., Celniker, A., Shah, V., Bowsher, R., Mire-Sluis, A., Findlay, J.W., Saltarelli, M., Quarmby, V., Lansky, D., Dillard, R., Ullmann, M., Keller, S., Karnes, H.T., 2005. Bioanalytical method validation for macromolecules in support of pharmacokinetic studies. Pharm Res 22, 1425-1431.

Spunt, S.L., Grupp, S.A., Vik, T.A., Santana, V.M., Greenblatt, D.J., Clancy, J., Berkenblit, A., Krygowski, M., Ananthakrishnan, R., Boni, J.P., Gilbertson, R.J., 2011. Phase I study of temsirolimus in pediatric patients with recurrent/refractory solid tumors. J Clin Oncol 29, 2933-2940.

Swerts, K., De Moerloose, B., Dhooge, C., Brichard, B., Benoit, Y., Laureys, G., Philippe, J., 2004. Detection of residual neuroblastoma cells in bone marrow: comparison of flow cytometry with immunocytochemistry. Cytometry B Clin Cytom 61, 9-19.

Vandewoestyne, M., Kumps, C., Swerts, K., Menten, B., Lammens, T., Philippe, J., De Preter, K., Laureys, G., Van Roy, N., Speleman, F., Deforce, D., 2012. Isolation of disseminated neuroblastoma cells from bone marrow aspirates for pretreatment risk assessment by array comparative genomic hybridization. Int J Cancer 130, 1098-1108.

Vervoorts, J., Luscher-Firzlaff, J., Luscher, B., 2006. The ins and outs of MYC regulation by posttranslational mechanisms. J Biol Chem 281, 34725-34729.

Workman, P., 2003. How much gets there and what does it do?: The need for better pharmacokinetic and pharmacodynamic endpoints in contemporary drug discovery and development. Curr Pharm Des 9, 891-902.

Yap, T.A., Yan, L., Patnaik, A., Fearen, I., Olmos, D., Papadopoulos, K., Baird, R.D., Delgado, L., Taylor, A., Lupinacci, L., Riisnaes, R., Pope, L.L., Heaton, S.P., Thomas, G., Garrett, M.D., Sullivan, D.M., de Bono, J.S., Tolcher, A.W., 2011. First-in-man clinical trial of the oral pan-AKT inhibitor MK-2206 in patients with advanced solid tumors. J Clin Oncol 29, 4688-4695.

Yap, T.A., Yan, L., Patnaik, A., Tunariu, N., Biondo, A., Fearen, I., Papadopoulos, K.P., Olmos, D., Baird, R., Delgado, L., Tetteh, E., Beckman, R.A., Lupinacci, L., Riisnaes, R., Decordova, S., Heaton, S.P., Swales, K., deSouza, N.M., Leach, M.O., Garrett, M.D., Sullivan, D.M., de Bono, J.S., Tolcher, A.W., 2014. Interrogating Two Schedules of the AKT Inhibitor MK-2206 in Patients with Advanced Solid Tumors Incorporating Novel Pharmacodynamic and Functional Imaging Biomarkers. Clin Cancer Res 20, 5672-5685.

Zirath, H., Frenzel, A., Oliynyk, G., Segerstrom, L., Westermark, U.K., Larsson, K., Munksgaard Persson, M., Hultenby, K., Lehtio, J., Einvik, C., Pahlman, S., Kogner, P., Jakobsson, P.J., Henriksson, M.A., 2013. MYC inhibition induces metabolic changes leading to accumulation of lipid droplets in tumor cells. Proc Natl Acad Sci U S A 110, 10258-10263.

Figure captions

Figure 1. Isolation of neuroblastoma cells by fluorescence activated cell sorting

(A) Flow cytometry dotplots of PBMCs and/or Kelly cells labelled with GD2-PE, CD56-FITC and CD45-APC H7 antibodies pre- and post- FACS sorting. High and low spiked samples were 1.5 $x10^6$ and 3 x 10^5 Kelly cells into 6ml whole blood, respectively. Thick black boxes indicate quadrants for isolated GD2+/CD56+/CD45- neuroblastoma cells. (B) The percentage of Kelly cells (GD2+/CD56+/CD45-) pre- and post- FACS cell sorting. The mean fold enrichment of Kelly cells from the spiked samples is indicated in brackets above the post bars. Mean±SD from 3 independent experiments. **p value<0.01, ***p value<0.001 by unpaired t test. (C) Recovery rates of Kelly cells by FACS cell sorting = (Number of Kelly cells collected from cell sorter/Total Kelly cells added to sample before sorting)x100, Mean±SD from 3 independent experiments. PBMC: peripheral blood mononuclear cells

Figure 2. Neuroblastoma cell enrichment from patient bone marrow aspirates

Bone marrow aspirates from neuroblastoma patients were sorted by FACS to isolate GD2+/CD56+/CD45- cells. (A) Example flow cytometry dotplots from a single bone marrow aspirate pre- and post-sorting. Thick black boxes indicate quadrants for GD2+/CD56+/CD45- neuroblastoma cells. (B) The percentage of neuroblastoma cells in 11 bone marrow samples pre- and post-sorting is plotted for patients in which GD2+/CD56+/CD45- cells were detected. Five post-sorted samples had ≤10,000 cells and purity was not determined (See Table 2).

Figure 3. An immunoassay to measure MYCN protein in neuroblastoma cells

(A) Titration of recombinant MYCN protein shows linearity in MYCN immunoassay. Mean±SD from 4 independent repeats. (B) MYCN protein levels in 6 neuroblastoma cell lines (3 with amplified *MYCN*) by immunoassay using 25µg or 10µg of total protein. Mean±SD of 3 independent repeats. (C) MYCN protein levels by western blot using cell

lysates from (B). (D) Western blot for AZD8055 treated Kelly cells (3h) showing a dose-dependent depletion of MYCN protein. (E) Quantitation of dose-dependent MYCN protein depletion levels by AZD8055 in Kelly cells by immunoassay. Mean±SD of 3 independent repeats. **p value<0.01, ***p value<0.001 compared with no treatment control by one-way ANOVA followed by Dunnett's multiple comparison test.

Figure 4. Measurement of MYCN protein in isolated neuroblastoma cells

(A) MYCN protein levels in pre- and post-sorted Kelly spiked PBMCs or PBMCs alone relative to Kelly cells alone in samples processed after 0, 1, 4 or 24 hours. Mean±SD from 3 independent experiments. **p value<0.01 compared with Kelly only by one-way ANOVA followed by Dunnett's multiple comparison test. (B) MCYN protein levels in Kelly cells isolated from spiked healthy volunteer blood and lysed and either frozen immediately at -80ºC or stored overnight on dry ice then frozen at -80ºC. Samples were analyzed by MYCN immunoassay after 1 day, 1 week or 4 weeks of storage. (C) Schematic of the suggested set up for bone marrow processing, transport, storage and biomarker measurement for MYCN protein analysis in a multi-site clinical trial context. (D) MYCN protein levels measured in immunoassay pre- and post- enrichment of Kelly neuroblastoma cells by FACS sorting using 5µg total protein per sample and compared with PBMC only samples. High and low spiked samples were 1.5 $x10^6$ and 3 x 10^5 Kelly cells into 6ml whole blood, respectively. Mean±SD from 3 independent experiments. *p value<0.05, ns=not significant by unpaired t test. (E) MYCN protein levels quantified by immunoassay for pre-sorted PBMCs with spiked Kelly cells (grey bars) or post-sorted spiked Kelly cells (black bars). Samples were untreated or treated for 3h with 5µM or 40 µM AZD8055 Mean±SD from 3 independent experiments. *p value<0.05, **p value<0.01, ns=not significant compared with no treatment control by one-way ANOVA followed by Dunnett's multiple comparison test.

Figure 5. Measurement of MYCN protein in patient bone marrow samples

Neuroblastoma cells were isolated from left (A) and right (B) bone marrow aspirates and MYCN protein expression analyzed by immunoassay. Equal amounts of total protein/well were used for each set of samples (20µg for 8R and 6µg for 8L) and lysates were run in duplicate. Pre-sorted bone marrow (grey bars) and post-sorted neuroblastoma cells (black bars) are compared with sorted white blood cells (white bars). (C) MYCN expression was confirmed in bone marrow from patient 8 by western blotting, with Kelly cell lysate used as a positive control for MYCN protein. (D) Neuroblastoma cells were isolated from bone marrow aspirates from three additional patients and MYCN protein expression analyzed by immunoassay. Equal amounts of total protein/well were used for each set of samples (as indicated) and lysates were run in duplicate. Pre-sorted bone marrow (grey bars) and post-sorted neuroblastoma cells (black bars) are compared with sorted white blood cells (white bars).

Figure 6. PI3K/AKT/mTOR pathway activity in platelet-rich plasma

(A) Phospho AKT (pS473), GSK3β (pS9), P70S6K (pT421/pS424) and (B) total AKT, GSK3β and P70S6K signals for 24 adult and 24 pediatric patient PRP samples detected using the MSD® triplex assay plates for phospho and total signals. ECL: Electrochemiluminescence. (C) Ratios of phospho over total protein levels for AKT, GSK3β and P70S6K for each patient shows the proportion of kinases that are active. Adult results are shown in grey and pediatric results in black. Mean values for each data set are shown above and represented by black bars. *p value<0.05, **p value<0.01 by unpaired two-tailed t test.

Table 1. Comparison of neuroblastoma isolation methods

Kelly cells were spiked into whole blood followed by Lymphoprep™ isolation of the peripheral blood mononuclear cell (PBMC) fraction. Results show flow cytometry analysis of Kelly cell populations pre- and post- neuroblastoma cell isolation techniques using CD56 positive selection (CD56 MACS microbeads), CD45 negative selection (CD45 MACS microbeads) or

3-color (APC-H7-CD45, PE-GD2 and FITC-CD56) fluorescence activated cell sorting (FACS). Mean±SD, n≥3

Table 2. Summary of neuroblastoma cell isolation from patient bone marrow

Patient bone marrow aspirates with detectable neuroblastoma infiltration were sorted by FACS. The level of neuroblastoma cells (CD45-/GD2+/CD56+) detected pre-sorting, fold enrichment following sorting and the total number of neuroblastoma cells collected is shown for each sample. Independent analysis of bone marrow infiltration was performed from bone marrow smears/trephine biopsies and results classed as 'No detection', 'Tumor cells detected' or 'Heavy infiltration'. The extent of bone marrow infiltration detected by flow cytometry is catergorized as follows: Very low <0.1%, Low >0.1-1%, Medium >1-10% and High >10%. ND=Not determined (due to very low cell numbers). Patients 1, 2, 3, 4, 7, 9 and 12 did not show any detectable bone marrow infiltration by FACS or independent analysis and so they are not presented here.

Figure 1

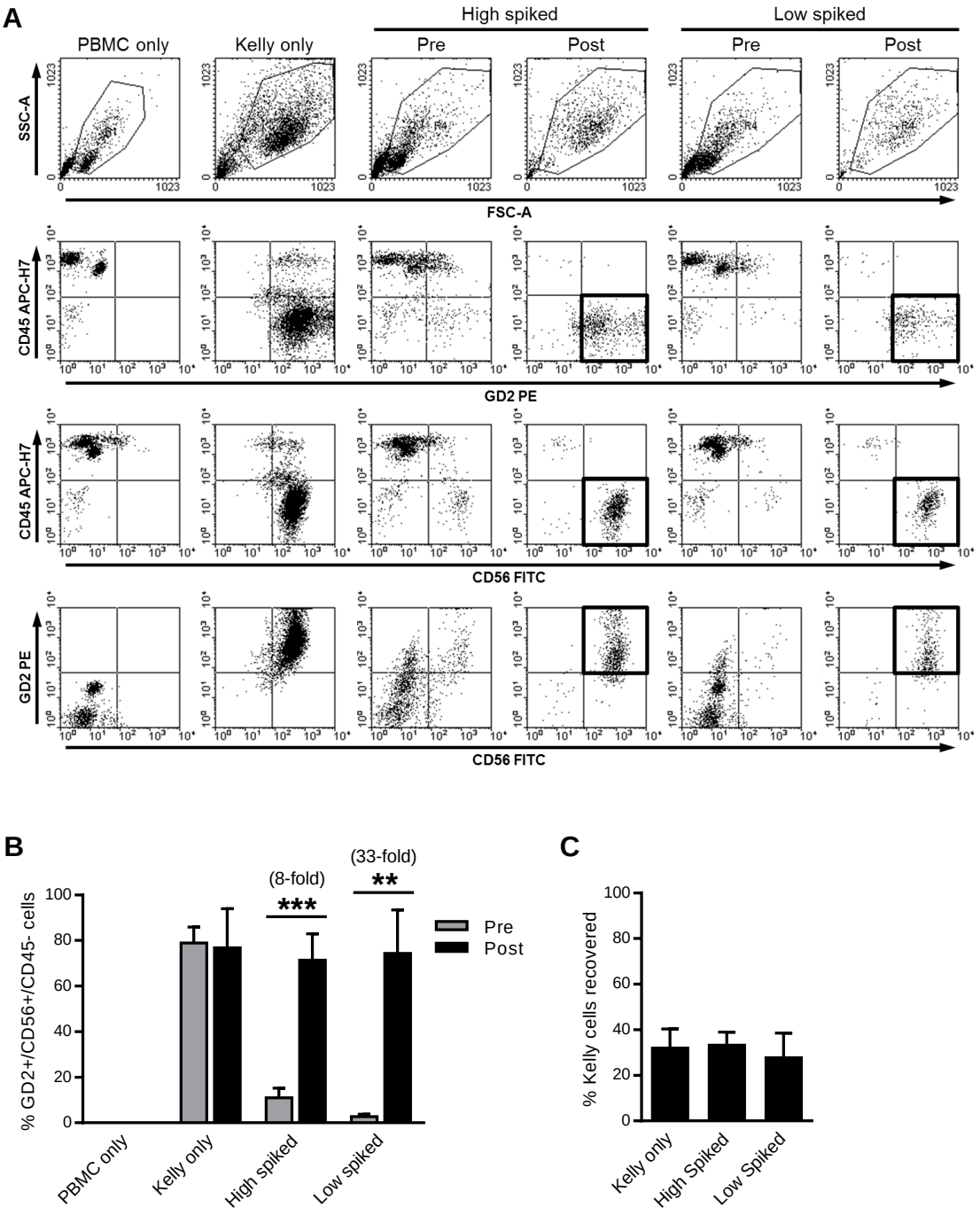
A
High spiked
Low spiked
PBMC only
Kelly only
Pre
Post
Pre
Post
SSC-A
FSC-A
CD45 APC-H7
GD2 PE
CD45 APC-H7
CD56 FITC
GD2 PE
CD56 FITC
B
(8-fold)
(33-fold)
***
**
Pre
Post
% GD2+/CD56+/CD45- cells
PBMC only
Kelly only
High spiked
Low spiked
C
% Kelly cells recovered
Kelly only
High Spiked
Low Spiked

Figure 2

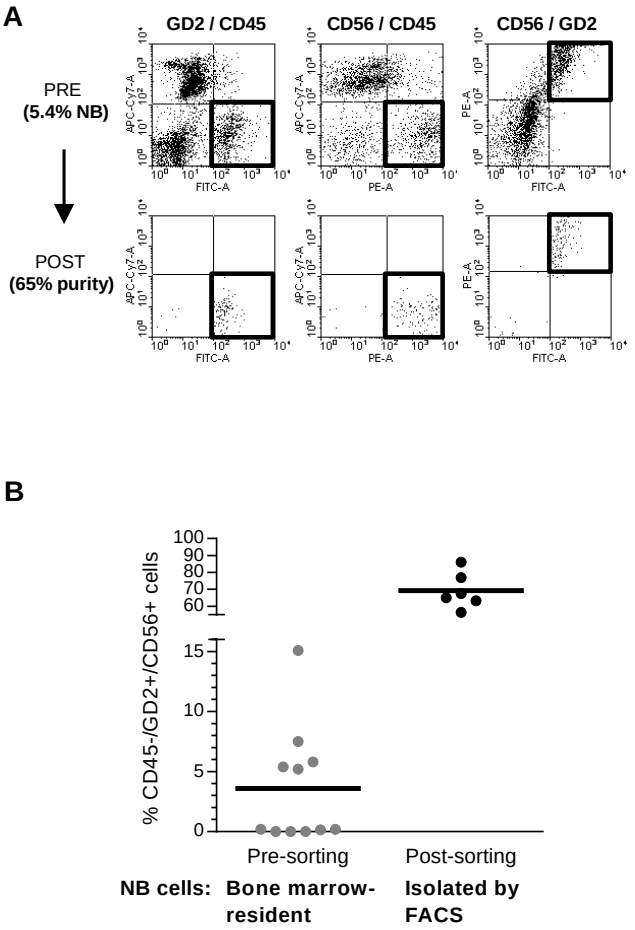
A
GD2 / CD45
CD56 / CD45
CD56 / GD2
PRE
(5.4% NB)
POST
(65% purity)
APC-Cy7-A
PE-A
FITC-A
B
% CD45-/GD2+/CD56+ cells
100
90
80
70
60
15
10
5
0
Pre-sorting
Post-sorting
NB cells: Bone marrow-resident
Isolated by FACS

Figure 3

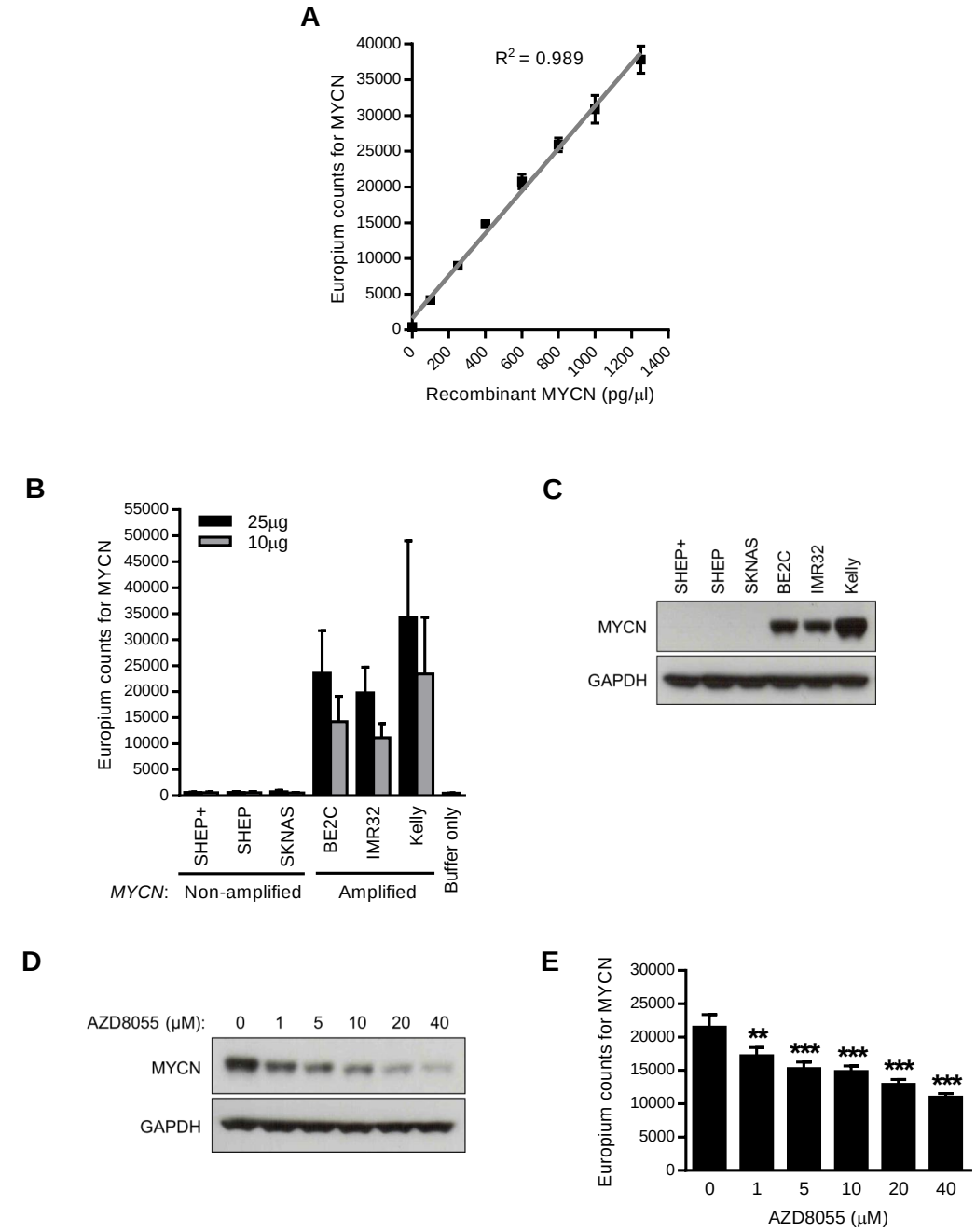
A
R2 = 0.989
Europium counts for MYCN
Recombinant MYCN (pg/µl)
B
25µg
10µg
Europium counts for MYCN
SHEP+
SHEP
SKNAS
BE2C
IMR32
Kelly
Buffer only
MYCN: Non-amplified
Amplified
C
SHEP+
SHEP
SKNAS
BE2C
IMR32
Kelly
MYCN
GAPDH
D
AZD8055 (µM): 0 1 5 10 20 40
MYCN
GAPDH
E
Europium counts for MYCN
AZD8055 (µM)

Figure 4

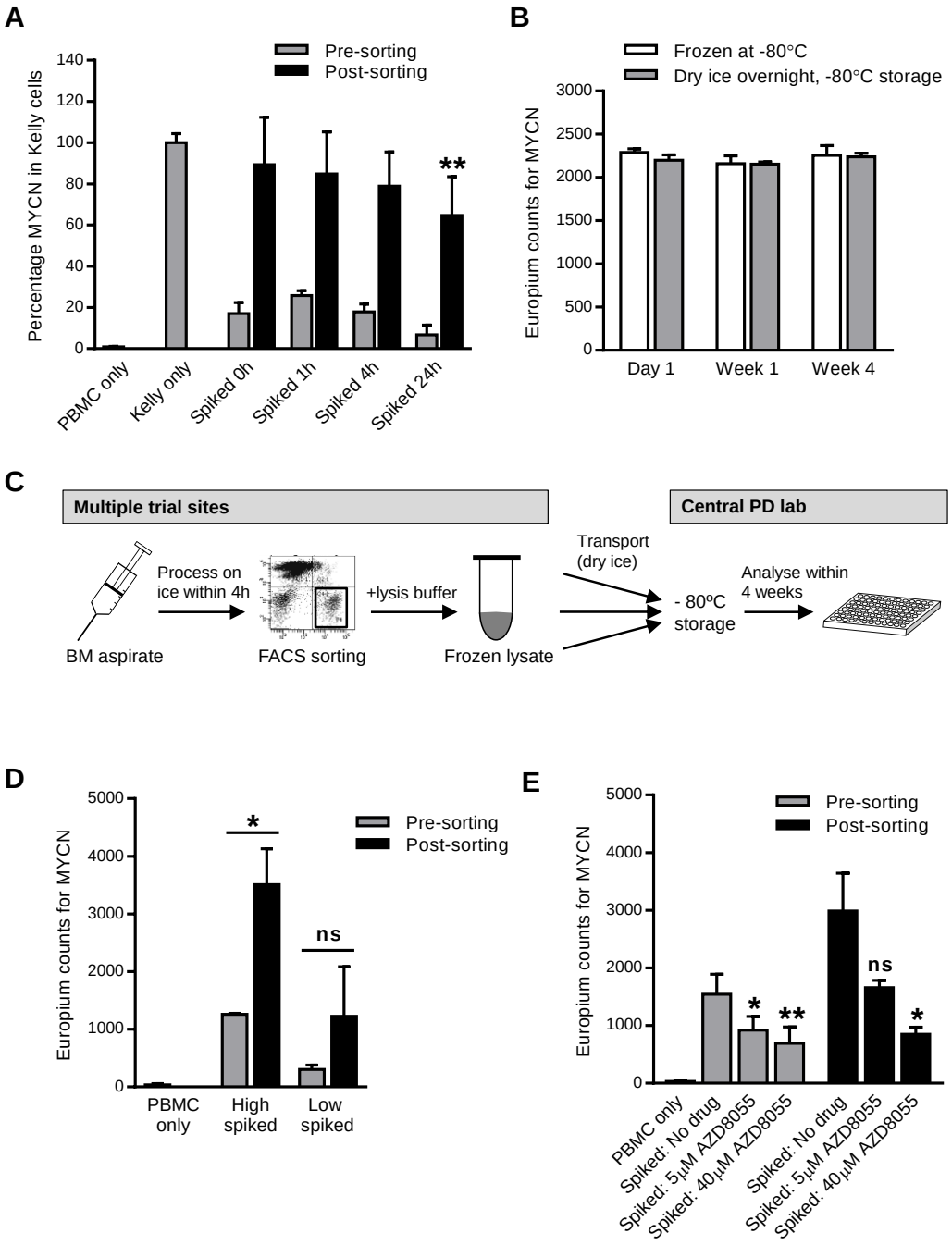
A
Pre-sorting
Post-sorting
Percentage MYCN in Kelly cells
140
120
100
80
60
40
20
0
**
PBMC only
Kelly only
Spiked 0h
Spiked 1h
Spiked 4h
Spiked 24h
B
Frozen at -80°C
Dry ice overnight, -80°C storage
Europium counts for MYCN
3000
2500
2000
1500
1000
500
0
Day 1
Week 1
Week 4
C
Multiple trial sites
Central PD lab
Process on ice within 4h
+lysis buffer
Transport (dry ice)
- 80ºC storage
Analyse within 4 weeks
BM aspirate
FACS sorting
Frozen lysate
D
Pre-sorting
Post-sorting
Europium counts for MYCN
5000
4000
3000
2000
1000
0
*
ns
PBMC only
High spiked
Low spiked
E
Pre-sorting
Post-sorting
Europium counts for MYCN
5000
4000
3000
2000
1000
0
*
**
ns
*
PBMC only
Spiked: No drug
Spiked: 5μM AZD8055
Spiked: 40μM AZD8055
Spiked: No drug
Spiked: 5μM AZD8055
Spiked: 40μM AZD8055

4

Figure 5

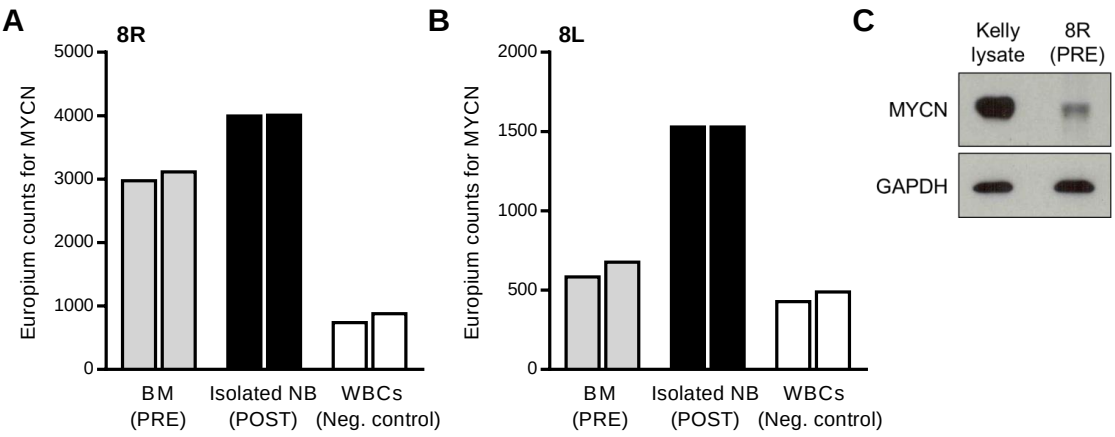
A
8R
Europium counts for MYCN
5000
4000
3000
2000
1000
0
BM (PRE)
Isolated NB (POST)
WBCs (Neg. control)
B
8L
Europium counts for MYCN
2000
1500
1000
500
0
BM (PRE)
Isolated NB (POST)
WBCs (Neg. control)
C
Kelly lysate
8R (PRE)
MYCN
GAPDH

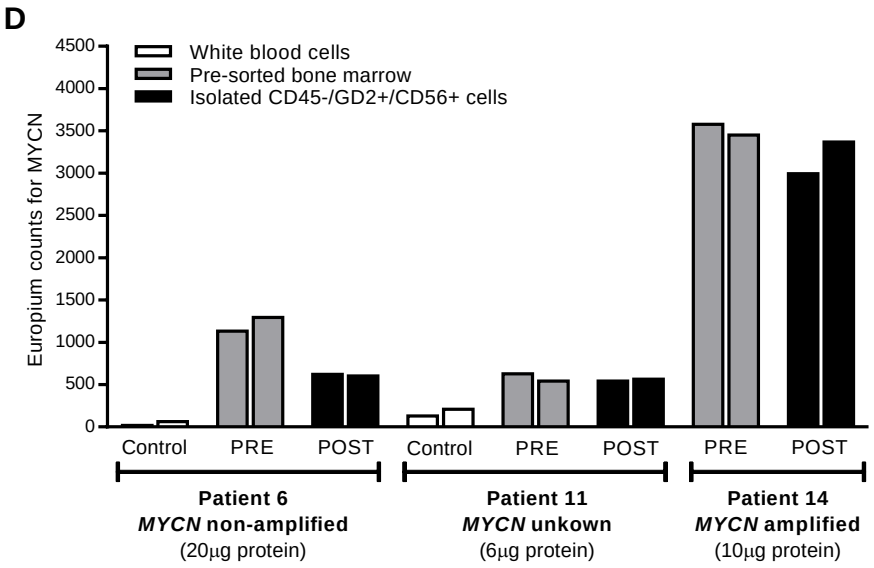
D
White blood cells
Pre-sorted bone marrow
Isolated CD45-/GD2+/CD56+ cells
Europium counts for MYCN
4500
4000
3500
3000
2500
2000
1500
1000
500
0
Control
PRE
POST
Control
PRE
POST
PRE
POST
Patient 6
MYCN non-amplified
(20μg protein)
Patient 11
MYCN unkown
(6μg protein)
Patient 14
MYCN amplified
(10μg protein)

Figure 6

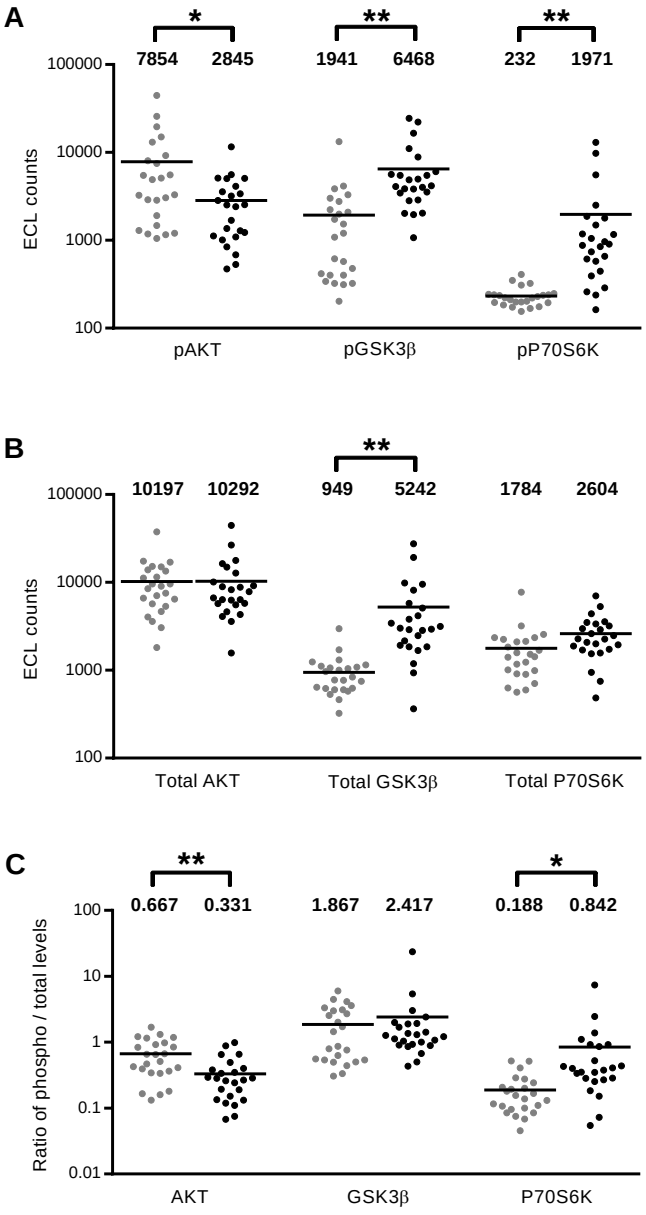
A
*
**
**
7854
2845
1941
6468
232
1971
100000
10000
1000
100
ECL counts
pAKT
pGSK3β
pP70S6K
B
**
10197
10292
949
5242
1784
2604
100000
10000
1000
100
ECL counts
Total AKT
Total GSK3β
Total P70S6K
C
**
*
0.667
0.331
1.867
2.417
0.188
0.842
100
10
1
0.1
0.01
Ratio of phospho / total levels
AKT
GSK3β
P70S6K

Table 1

		Kelly cells		
Isolation technique	**Selection marker(s)**	**% PRE**	**% POST**	**Fold enrichment**
Immunomagnetic beads	CD56 positive	16.0 ±3.3	26.8 ±5.0	1.7 ±0.3
Immunomagnetic beads	CD45 negative	14.6 ±3.8	58.2 ±28.2	3.9 ±1.3
FACS	GD2/CD56 positive, CD45 negative	15.0 ±1.4	80.5 ±3.7	5.4 ±0.7

Table 2

Patient	*MYCN* status	BMA sample	Detection of bone marrow resident neuroblastoma cells		Post-sorting	
			Level by flow cytometry	Confirmation by morphology/ICC?	Fold enrichment	Estimated cell number isolated
5	Amplified	Left	Very low	No detection	ND	1000
		Right	Very low	No detection	ND	1100
6	Non-amplified	Left	Very low	ND	ND	1500
		Right	Medium	Heavy infiltration	11.5	470000
8	Non-amplified	Left	Medium	Heavy infiltration	12.0	785000
		Right	Medium	Heavy infiltration	10.9	605000
10	Amplified	Unknown	Low	Tumor cells detected	ND	10000
11	Unknown	Right	High	Heavy infiltration	3.7	2190000
13	Amplified	Left	Low	Tumor cells detected	337.5	26000
		Right	Low	Tumor cells detected	ND	6500
14	Amplified	Left	Medium	Heavy infiltration	14.8	266000